TOWARDS AN AUTONOMOUS VTOL-MAV BY INTEGRATION OF IMAGE BASED NAVIGATION

N. Frietsch, C. Keßler, O. Meister, J. Seibold, and G. F. Trommer
Institute of Systems Optimization
University of Karlsruhe (TH)
Kaiserstr. 12, 76128 Karlsruhe

ABSTRACT

This paper focuses on the development of an autonomous small-scale four rotor VTOL-MAV. The on-board GPS/INS navigation system has been augmented by further sensors in order to allow for an autonomous waypoint mode. Especially in urban environments the GPS signal quality is disturbed by shading and multipath propagation. In these cases, the investigated vision system based on algorithms analyzing the optical flow is essential to enable the helicopter to reliably hover. In order to enable a robust autonomous landing mode, the height above ground is estimated from the relative altitude change given by the barometric altimeter and the optical flow.

1. INTRODUCTION

The research activity in the field of unmanned micro aerial vehicles (MAV) has significantly increased over the last few years. Their application area ranges from rather basic tasks like the collection of sensor data to more and more complex utilizations in security and rescue operations. Their use in cases of industrial or natural disasters like for example earthquakes can significantly reduce the risk for human rescue teams, as an on-board digital camera acquires important information about the observed situation. In most of these scenarios the capacity to hover and fly autonomously along a specified path is essential. This article focuses on the augmentation of a small, electrically powered MAV with vertical take-off and landing (VTOL) capabilities with a vision based system.

Increased autonomy of MAVs poses demanding challenges concerning the navigation and guidance algorithms. Their navigation systems often depend on GPS information, what may cause problems especially in urban environments as GPS coverage and signal quality decrease due to shading and multipath effects. As MAVs have in the scenarios described above image sensors as payload on-board, especially vision based navigation systems have been investigated with promising results to overcome this shortcoming. In case the infrastructure is available, one possibility is to use geo-referenced aerial images as reference for the on-board images. Conte and Doherty presented an image based navigation system including visual odometers and on-board image registration to geo-referenced aerial images [1]. For the case when only the on-board sensor information is available, the critical situations of hovering and landing have been studied in particular. A lot of work has been done on the landing on a helicopter landing pad with known size, shape, and texture with great results [2] [3] [4]. The flatness of the landing pad is taken into account. Similarly, Caballero et al. calculate the motion of a mono-camera from views of a planar patch by estimating homographies in order to hover in front of buildings [5]. For the measurement of the distance to the ground several sensors like stereo vision, ultrasonic sonar, or radar were investigated.

Fig. 1. Four rotor MAV platform in flight.

In the following, we present our current work on a vision based navigation system for the VTOL-MAV shown in Figure 1. The relative camera motion from frame to frame is modeled by homographies. Therefore, the system is especially useful for the situations of hovering and landing as during the landing phase the assumption of a planar scene and during a hovering scenario the assumption of very little translational motion holds. It enhances the system also during translational flight if the camera observes a rather flat scene, what is mostly the case if the camera is mounted perpendicular under the helicopter.
No known structure in the ground plane and no absolute distance sensor are necessary. The height above ground is estimated only from the optical flow

extracted from the images of an on-board mono-camera and the data from an on-board barometric pressure sensor. A similar approach for the height estimation has been used by Barber et al. during the landing phase of a small fixed-wing UAV [6]. In contrast to our work, they used an optical flow sensor with fixed update-rate. With our approach, we can adjust the update rate of the optical flow calculation by varying the time between the used image frames. As the optical flow is slower the larger the distance from the camera to the image scene is, this has shown to be essential for a good accuracy of the height measure.

This paper is organized as follows: In Section 2, the VTOL-MAV and its navigation and guidance modules are described briefly followed by the definitions of the used coordinate systems in Section 3. The image processing algorithms for the image based motion and height above ground estimation are outlined in Section 4. Section 5 comprises the software-in-the-loop simulation environment being essential for the design and test of the navigation and guidance algorithms. In Section 6, the performances of the developed and implemented algorithms are illustrated followed by a conclusion.

2. VTOL-MAV PLATFORM

The developed four-rotor VTOL-MAV is shown in Figure 1. It has a maximum diameter of 92 cm and a take-off weight of below 1 kg including the payload capacity of 200 g. This light weight has been chosen deliberately to ensure operation without legal restrictions in order to allow the instantaneous operation of the MAV at any time.
Due to severe restrictions on weight, cost, and power consumptions only low quality sensors can be used. Therefore, the MAV is equipped with an on-board navigation system that integrates the different sensor data. The system determines the position, velocity, and attitude of the helicopter and bases on the integration of a three-axes MEMS-IMU (Micro-Electro-Mechanical System, Inertial Measurement Unit) with a GPS receiver. If in case of GPS signal loss the navigation solution based solely on the MEMS-IMU sensors, it would be only accurate for a short time and diverge almost instantaneously. Therefore, the system is augmented by a barometric height sensor improving the relative altitude estimation and a three-axes magnetometer that stabilizes together with a model of the earth's magnetic field the yaw angle of the MAV [7]. This is also mandatory during hovering flight when the yaw angle becomes unobservable in a GPS/INS system. For the integration of the sensor data an error state space Kalman filter, also known as indirect Kalman filter, with 16 states is used. The state vector comprises the three errors of the position, the three errors of the velocity, the three errors of the attitude as well as the errors of the biases of the three accelerometers, the errors of the biases of the three gyroscopes and the error of the bias of the barometric altimeter in order to be able to correct the sensor information. The estimated quantities as well as the sensor data and some status information of the MAV are stored on-board on a flight recorder and can be analyzed after the flight.

The described navigation system together with the cascaded controllers and suitable guidance algorithms allow the operation of the MAV in the semi-autonomous "position hold" mode as well as the autonomous "waypoint" flight mode [7]. The position hold mode is a completely self stabilized hovering mode. The small aircraft keeps its three-dimensional position fixed and autonomously compensates disturbances due to wind. In the waypoint flight mode, the MAV is additionally capable to follow autonomously a pre-defined trajectory. This allows autonomous flights outside the range of sight and outside the range of the radio link. Both modes depend on position information and without the aid of the vision system have therefore only been applicable if GPS signals of good quality were available. In order to automate the step of the trajectory planning, global preflight path planning has been investigated [8].

With its hovering capabilities, the MAV is especially useful for the acquisition of aerial image data providing important information about the observed scene. Therefore, a digital camera is mounted as payload on the chassis under the center of the mass of the MAV. An automated processing of the images is useful to support the human operator. In a catastrophe scenario for example, the knowledge of the coordinates of detected objects with respect to a geo-referenced coordinate system is indispensable for the efficient coordination of the rescue teams. Furthermore, the image data is used to augment the autonomy of the MAV for example by extracting navigation information and integrating it in the on-board navigation system.

3. DEFINITIONS OF COORDINATE SYSTEMS

In this section, the coordinate systems and definitions being used in the following are described:
The on-board navigation system estimates the attitude, the position, and the velocity of the MAV. The attitude describes the rotation between the body-fixed coordinate system (denoted by index b) and the so-called navigation coordinate system (denoted by index n) pointing in a northward, eastward, and downward direction. The attitude can be expressed with the three Euler angles $(\phi_{nb}, \theta_{nb}, \psi_{nb})$ (see Fig. 2) or the direction cosine matrix $\mathbf{C}_{n,b}$ being especially useful for coordinate transformations.

The MAV's position $\vec{x}^{\,e}_{\mathrm{MAV}}$ is expressed in the navi-

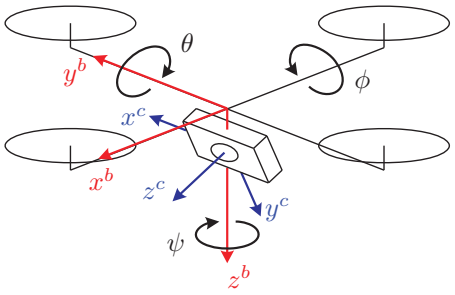

Fig. 2. Definitions of Euler angles as well as body-fixed and camera coordinate systems.

gation system in ECEF-coordinates (Earth-Centered Earth-Fixed)[1]. Due to the operating range of the helicopter of some kilometers, the earth's surface can be approximated by its tangent plane with fixed attitude $C_{n,e}$. For simplification, the position of the MAV is in the following expressed as the differential position $\Delta\vec{x}^{\,n}_{\mathrm{MAV}}$ from the helicopter's initial position $\vec{x}^{\,e}_{\mathrm{MAV,init}}$ with coordinates in northward, eastward, and downward direction

$$\Delta\vec{x}^{\,n}_{\mathrm{MAV}} = C_{n,e} \cdot \left(\vec{x}^{\,e}_{\mathrm{MAV}} - \vec{x}^{\,e}_{\mathrm{MAV,init}}\right). \tag{1}$$

The attitude between the camera and the helicopter is supposed to be fixed and can be described by the three angles $(\phi_{bc}, \theta_{bc}, \psi_{bc})$ or $\mathbf{C}_{b,c}$. The definitions of the body coordinate system and the camera coordinate system are visualized in Fig. 2 with the optical axis of the camera pointing towards ground. In the following, the centers of body and camera coordinate systems are supposed to coincide. The attitude between camera and helicopter is estimated before the flight and is supposed to be fixed.

4. VISION BASED MOTION ESTIMATION

The described vision based estimation of the motion of the camera and therefore also of the MAV depends on the processing of homographies what is suitable, if the camera observes a planar scene or if only rotational motion occurs. Therefore, the system is especially useful during hovering situations, but it enhances the performance also during translational flight and during the landing phase if the camera observes a rather flat scene, what is mostly the case if the camera is mounted perpendicular under the helicopter.

4.1. Homography Estimation

The homography estimation bases on point-to-point correspondences between subsequent images that have been extracted with the well known iterative Lucas-Kanade-algorithm [9]. This algorithm bases on the assumption that all pixel in a small neighborhood are subject to the same optical flow. It works best at points having a neighborhood with high intensity variances [10]. Therefore, points are selected in the first frame with a Harris-corner-detector [11] and the strongest corners are kept for registration. Then their positions in the subsequent frame are calculated with subpixel accuracy by applying the iterative Lucas-Kanade-algorithm on different image resolution levels. For the homography estimation, around 200 points are selected in the first frame. By dividing the image into small parts and choosing the strongest points within each, the points are reasonably distributed over the whole image plane what is essential for a good homography estimation.

Under the assumption that the observed scene is planar or the motion of the camera is pure rotational, the geometrical relation between the consecutive frames $\mathbf{F}_k$ and $\mathbf{F}_{k+1}$ can be described by the homography matrix $\mathbf{H}_{k+1,k}$. The relation is given by

$$\vec{x}_{k+1} \sim \mathbf{H}_{k+1,k} \cdot \vec{x}_k, \tag{2}$$

with the homogeneous coordinates $\vec{x}_k$ of the pixels in frame $\mathbf{F}_k$ and $\vec{x}_{k+1}$ of the corresponding pixels in frame $\mathbf{F}_{k+1}$, respectively. To estimate the eight degrees of freedom of the homography matrix, at least four known point correspondences are necessary, but to increase robustness and accuracy all correspondences being computed by the optical flow algorithm are used. The coordinates of the found point pairs are normalized by isotropic scaling [12]. Additionally, the robust RANSAC algorithm [13] is used to find a subset of feature pairs resulting in a homography matrix that most points go well with. During this iterative process, points are identified that do not fit to the homography model. These outliers are mismatched feature pairs, points in the image where the planarity assumption does not hold or points belonging to moving objects in the scene. They need to be discarded as they significantly corrupt the estimation.

4.2. Homography Based Motion Estimation

If homography matrices are suitable for the description of the scene, the camera motion between the two frames $\mathbf{F}_k$ and $\mathbf{F}_{k+1}$ can be extracted from $\mathbf{H}_{k+1,k}$ as described by several authors like Triggs [14] or Ma et. al. [15]:
In the first step, the calibrated homography is calculated with the help of the camera calibration matrix $\mathbf{K}$ containing the intrinsic camera parameters [12]:

$$\mathbf{H}_{cal} = \mathbf{K}^{-1}\mathbf{H}\mathbf{K}, \tag{3}$$

with $\mathbf{H} = \mathbf{H}_{k+1,k}$. The calibrated homography can then be rewritten as

$$\mathbf{H}_{cal} = \pm\lambda \left(\mathbf{C}_{c_{k+1},c_k} + \frac{1}{d_k}\, \vec{t}^{\,c_{k+1}}_{c_{k+1},c_k}\, \vec{n}^{\,c_k\,T}\right). \tag{4}$$

[1] In the following the superscript character after a variable specifies the coordinate system with respect to which the variable is given.

with λ being the second-largest singular value of $\mathbf{H}_{cal}$. Furthermore $\mathbf{C}_{c_{k+1},c_k}$ is the direction cosine matrix from the camera coordinate system c_k at time k to the camera coordinate system c_{k+1} at time $k+1$; d_k is the distance from the center of the camera coordinate system at time k to the observed 2D-plane P in the real world. The translational displacement between the origins of the camera coordinate systems c_k and c_{k+1} is given by $\vec{t}^{\,c_{k+1}}_{c_{k+1},c_k}$ and $\vec{n}^{c_k}$ is the normal vector of the plane P given in coordinates of the camera coordinate system c_k. The sign of $\mathbf{H}_{cal}$ needs to be chosen so that for all corresponding homogeneous point pairs $\vec{x}_k$ and $\vec{x}_{k+1}$ in the images $\mathbf{F}_k$ and $\mathbf{F}_{k+1}$ the inequality

$$\vec{x}_{k+1} \cdot \mathbf{K} \cdot \mathbf{H}_{cal} \cdot \mathbf{K}^{-1} \cdot \vec{x}_k > 0 \tag{5}$$

holds. Only point pairs that have been classified as inliers of the homography estimation are considered. With the singular value decomposition of $\mathbf{H}_{cal}$ four solutions for the decomposition into $\mathbf{C}_{c_{k+1},c_k}$, $\frac{1}{d}\vec{t}^{\,c_{k+1}}_{c_{k+1},c_k}$, and $\vec{n}^{c_k}$ can be calculated [14] [15]. Under the assumption that the observed points in the real world need to be situated in front of the cameras, only two of these solutions are physically possible. To obtain a single solution, the additional assumption is made that the helicopter is orientated mostly parallel to the ground plane P. Therefore, the solution with the normal vector $\vec{n}^n = (\mathbf{C}_{n,b_k}\mathbf{C}_{b_k,c_k}\vec{n}^{c_k})$ having the largest down-component is chosen, with b_k refering to the body coordinate system at time k. As the attitude from camera to body-fixed coordinate system is supposed to be fixed, the constant direction cosine matrices $(\mathbf{C}_{b_k,c_k} = \mathbf{C}_{b,c})$ and $(\mathbf{C}_{c_k,b_k} = \mathbf{C}_{c,b})$ are used in the following.

Having now identified the change of attitude and position of the camera between the two image acquisitions, the attitude and the position of the MAV are given according to the definitions in Section 3.3. by

$$\mathbf{C}_{n,b_{k+1}} = \mathbf{C}_{n,b_k}\mathbf{C}_{b,c}\mathbf{C}_{c_k,c_{k+1}}\mathbf{C}_{c,b} \tag{6}$$

and

$$\Delta\vec{x}^{\,n}_{\mathrm{MAV},k+1} = \Delta\vec{x}^{\,n}_{\mathrm{MAV},k} - \mathbf{C}_{n,b_k}\mathbf{C}_{b,c}\mathbf{C}_{c_k,c_{k+1}}\vec{t}^{\,c_{k+1}}_{c_{k+1},c_k} \tag{7}$$

with $\mathbf{C}_{c_k,c_{k+1}} = \mathbf{C}^T_{c_{k+1},c_k}$. For the absolute position estimation, the height above ground d_k at time k needs to be known. This can be either measured by a distance sensor or estimated as described in the next section. If the initial attitude $\mathbf{C}_{n,b_0}$ and position $\Delta\vec{x}^{\,n}_{\mathrm{MAV},0}$ of the MAV at the time of the first image acquisition is given by the on-board navigation system, the attitude and position are iteratively estimated over time with the help of the on-board images. The performance of the described method is evaluated in Section 6.

4.3. Vision Based Height Above Ground Estimation

In order to enable an autonomous landing of the helicopter, the information about the distance to the ground is essential. The on-board barometric altimeter gives the height differences from the start position of the helicopter. As these measurements are corrupted by a drift and additionally the height of the start and landing place of the MAV can differ significantly, this information is not sufficient. Due to the severe weight limitations no additional distance sensor can be carried on-board. The used approach is therefore the estimation of the height above ground from the optical flow between subsequent images and the relative change in height. The basic idea is sketched in Fig. 3. A camera is acquiring images from a scene parallel to the image sensor. Two points in

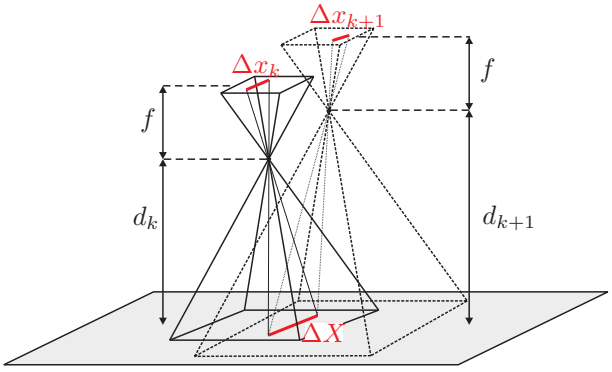

Fig. 3. Estimation of the height above ground from point correspondences and the difference in height.

the real world with the distance ΔX are projected on the sensing element of the camera at time k and have there the distance Δx_k. Under the assumption of a pinhole camera model, the theorem on intersecting lines leads to the equation

$$\frac{d_k}{\Delta X} = \frac{f}{\Delta x_k} \tag{8}$$

or

$$d_k = f \cdot \Delta X \cdot \frac{1}{\Delta x_k} \tag{9}$$

with the distance f from the camera's projection center to the image sensor and the distance d_k from the projection center to the image scene. Combining this with the same equation for time $k+1$ results in

$$\Delta d_{k,k+1} = d_{k+1} - d_k = f \cdot \Delta X \cdot \left(\frac{1}{\Delta x_{k+1}} - \frac{1}{\Delta x_k}\right) \tag{10}$$

and

$$d_{k+1} = f \cdot \Delta X \cdot \frac{1}{\Delta x_{k+1}} = \frac{\Delta d_{k,k+1}}{1 - \frac{\Delta x_{k+1}}{\Delta x_k}}. \tag{11}$$

The on-board barometric altimeter gives the height differences $\Delta d_{k,k+1}$ of the camera's principal point at different times and several pixel differences Δx_k and

Δx_{k+1} can be calculated from the point correspondences of the optical flow.
Reliable estimations of the height above ground based on this equation can only be achieved when vertical motion of the camera occurs. A simple Kalman filter is used to bridge the time between the irregular measurements. In the prediction step, the differences between the barometric measurements are processed as known inputs. Furthermore, the influence of the attitudes of the cameras need to be removed from the pixel correspondences as Eq. (11) only holds if both camera coordinate systems are perpendicular to the scene. Horizontal motion does not affect the estimation as long as point correspondences can still be found. More details and results have been presented in [16].

5. Simulation Environment

All algorithms concerning the navigation, guidance, and control of the helicopter have been developed and tested with the help of a software-in-the-loop simulation environment. This versatile tool allows the fast and simple validation of new algorithms. Additionally, it enables the detailed comparison of different strategies to solve a certain task. Results are especially significant as the simulation environment allows the testing of each strategy under the same reproducible conditions. Furthermore, original C code of the helicopter can be embedded and tested by using the software environments MATLAB® and Simulink® from *The MathWorks, Inc.*.

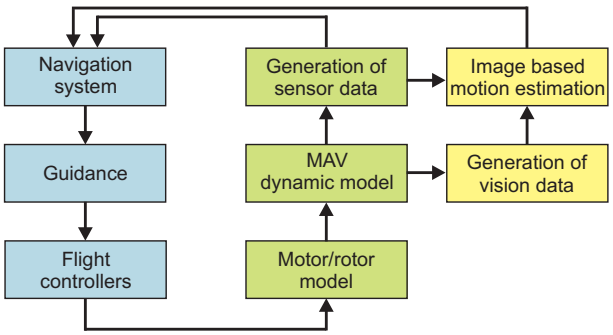

Fig. 4. Structure of the MAV simulation environment: Blocks with C Code are shown in blue. Blocks concerning the helicopter model are shown in green and blocks related to the developed image based navigation system are shown in yellow.

To close the control loop, a good model of the physical properties of the helicopter and of the influence of its environment is mandatory to replace the control process. In order to achieve significant results, the model parameters of the dynamic model like the inertia have been estimated with an identification process based on logged in-flight data and measurements. The structure of the simulation environment is shown in Fig. 4.
The position, velocity, and attitude being determined by the MAV dynamic model block are considered to be the ground truth for the simulation. With sensor errors like biases and scale factors that have been measured from the real sensors, realistic sensor data is generated from this ideal navigation solution and is used as input to the navigation block. The application of position hold and waypoint mode in the simulation is enabled by using the original guidance and flight control modules.
The algorithms of the vision based motion and the height above ground estimation, described in Section 4, are also included in the simulation. From the ideal navigation solution of the helicopter and an eligible attitude $\mathbf{C}_{b,c}$ between the virtual camera and the helicopter, the field of vision is calculated. At the beginning, an adjustable number of features are randomly distributed over the image plane. They are projected on the virtual earth surface and their coordinates are stored in a database. In the following time steps, the database is searched for features being still visible in the virtual image frame. To represent the real image processing module more precisely, scalable noise is added to the ideal, artificial features. From the extracted point correspondences the homography matrix is estimated and the motion from camera and helicopter is reconstructed as described in Section 4. If necessary, new features are generated and added to the database.

6. RESULTS

The performance of the described algorithms is discussed on the basis of simulation results as well as of first results of the processing of real in-flight data in this section.
For the development and test of the image based algorithms several waypoint flights of different lengths and heights were planned and simulated. The image rate was set to 25 frames/s and the image size was 640x480 pixels. Around 200 features were used and noise with zero mean and a standard deviation of σ = 1/3 pixel was added to the pixel positions in the optical flow module. The virtual camera was active above a height of 30 cm.
For the vision based data integration it was more promising to use the change of position and attitude and not the concatenated position and attitude measurements given by Eq. (6) and Eq. (7), as errors in the measurements sum up and can not be corrected. By dividing the differences of the angles or the positions by the image sampling time, the mean angular rates and the mean velocities of the MAV during the sampling time were determined. During the tests, the image based velocity estimation was integrated in the navigation filter in a measurement step.
The results of a simulated waypoint-flight of around 10 minutes are shown. The different position estimations along with the ground truth and the estimation errors of the positions are shown in Fig. 5. The

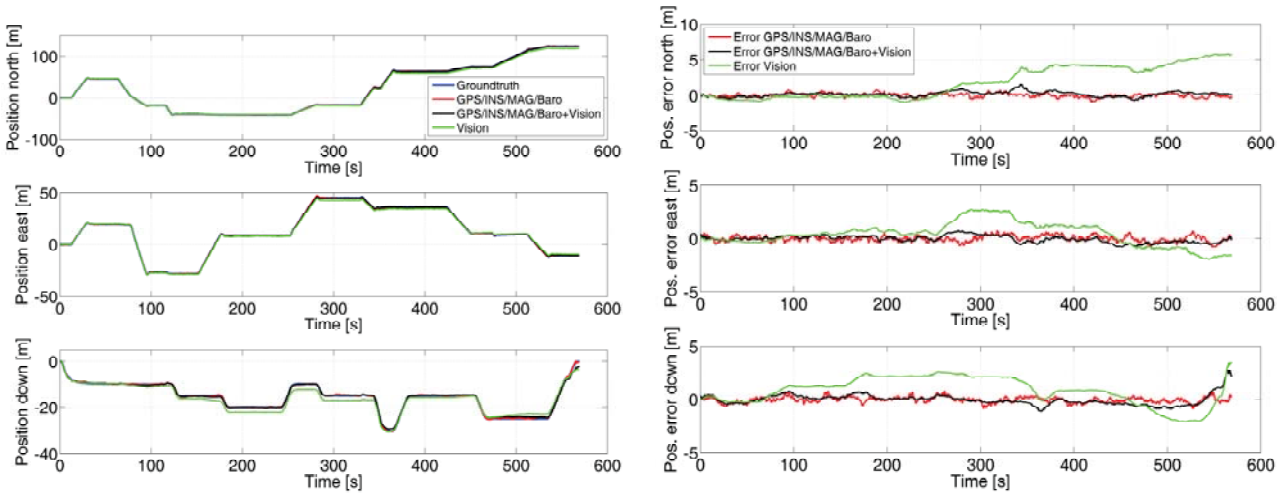

Fig. 5. Ground truth and position estimations of simulated waypoint flight in north, east and down coordinates as well as the errors of the position information.

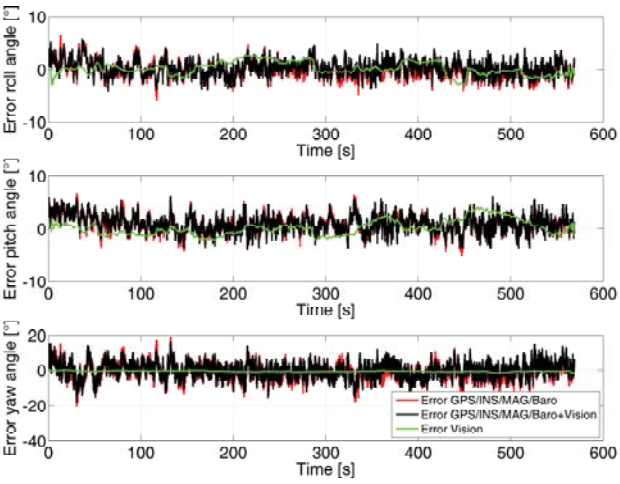

Fig. 6. Errors of attitude estimation of simulated waypoint flight.

estimation errors of the attitude are visualized in Fig. 6 including the estimation from the current onboard navigation system, the results of the additional integration of the vision based information as well as the concatenated measurements solely from the image based system. It is visible that the integrated navigation solution from the homography based motion estimation module gives similar good results as the GPS/INS Kalman filter. The pure vision based information is subject to drift.

In Fig. 7, the results of the height above ground estimation of this waypoint-flight are shown. The absolute error is after the processing of the first few measurements below 0.5 m. The Kalman filter for the height above ground estimation can be initialized with zero or alternatively with the sensor data from the barometric sensor. As soon as the first measurements from the vision based system are available, the filter converges to these height above ground measurements. At times when not enough vertical motion occurs, the filter propagates with the differential data of the barometric sensor. In the next step, the estimated height above the ground can be processed in the guidance module as difference to the set height if the landing of the MAV is desired.

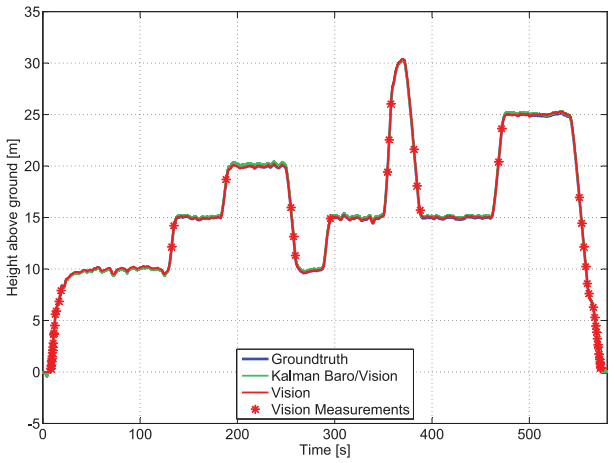

Fig. 7. Height above ground estimation of waypoint flight.

In the next step a GPS outage was simulated and the performance of the navigation filter with vision based enhancement was evaluated. Without the vision system, the horizontal position states diverge in a few seconds. The resulting position error during a GPS outage of 300 seconds are shown in Fig. 8. The simulation results indicate that GPS outages can be bridged with the image based position information.

The first step towards the evaluation of the performance of the developed algorithms in real flight was the post-processing of logged data. For this purpose, a flight has been accomplished and all sensor and navigation data as well as some status information

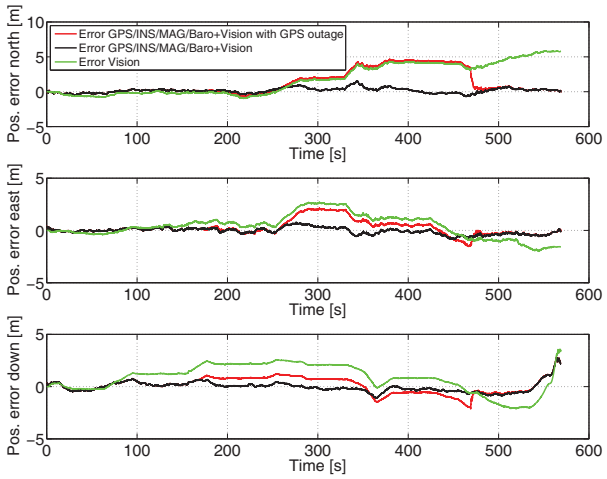

Fig. 8. Errors of position estimation with GPS outage from 175 s to 475 s. For comparison the performance without GPS outage is shown, too.

of the MAV has been logged by the flight recorder. Furthermore, the image stream was compressed and stored with VGA-resolution by the used off-the-shelf digital camera. The release of the camera by remote control during flight was logged by the flight controller of the MAV. On the ground station, the image data was then synchronized with the flight data. The whole flight was conducted over flat terrain in order to be in line with the assumptions of the use of homographies. The results of the height above ground estimation are shown in Fig. 9 together with the negative position estimation in down-direction of the on-board navigation system. This filter relies mostly on the barometric sensor data, as the height provided from GPS is most of the time erroneous. As the terrain was very flat, the relative height from the initial position of the MAV and the distance to the ground are the same during the whole flight. The camera was released 22 seconds after the start.

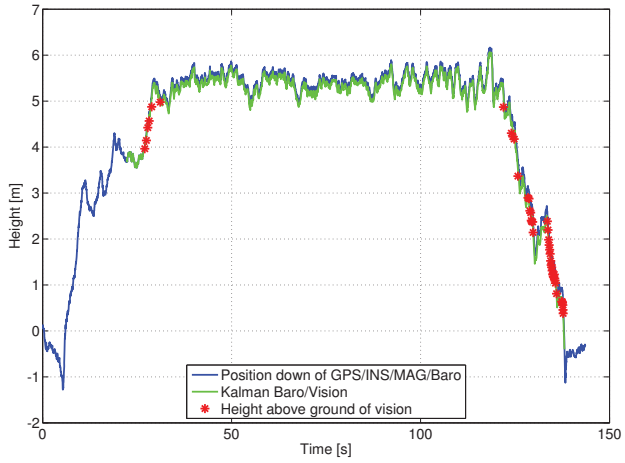

Fig. 9. Height above ground and estimation from in-flight data.

Due to the small size and weight of the aircraft, the on-board processing power has been limited and restricted so far to navigation and guidance purposes without image processing algorithms. Currently, a hardware platform is under development that will enable the calculation of basic image processing algorithms on-board in the near future.

7. CONCLUSION

In this paper, first results of an image based navigation system for a VTOL-MAV have been presented. Especially during landing and hovering situations, the MAV's attitude and position can be estimated using on-board image data. The described approach uses the optical flow extracted from the images as well as differential height information. This has the advantage that no structure in the ground plane and no absolute distance sensor are needed. The algorithms were tested with a software-in-the-loop simulation environment that represents the behavior of the helicopter very well. First results of the integration of the image based data into the GPS/INS navigation filter have shown that the navigation solution can be improved in case of bad GPS signal quality or even substitute the GPS information in case of short GPS outages. Different integration methods for the navigation filter are currently evaluated and compared. The first evaluation of the performance with in-flight data has shown promising results. A structured underground is important to enable precise optical flow estimation. Future work is the implementation of the image based navigation system on an on-board hardware platform and the detailed evaluation of the in-flight performance.

ACKNOWLEDGEMENTS

N. Frietsch thanks the Deutsche Telekom Stiftung for their sponsorship.
The authors wish to thank the microdrones GmbH.

8. REFERENCES

[1] Conte G., Doherty P., "An Integrated UAV Navigation System Based on Aerial Image Matching," in *Proceedings of the IEEE Aerospace Conference*, 2008.
[2] Shakernia O., Ma Y., Koo T. J., Sastry S., "Landing an unmanned air vehicle: Vision based motion estimation and nonlinear control," *Asian Journal of Control*, vol. 1, 1999.
[3] Sharp C. S., Shakernia O., Sastry S. S., "A vision system for landing an unmanned aerial vehicle," in *Proceedings of the 2001 ICRA. IEEE International Conference on Robotics and Automation*, vol. 2, 2001, pp. 1720 – 1727.
[4] Saripalli S., Sukhatme G. S., Montgomery J. F., "An experimental study of the autonomous helicopter landing problem," in *Proceedings of the International Symposium on Experimental Robotics*, 2002, pp. 466 – 475.
[5] Caballero F., Merino L., Ferruz J., Ollero A., "A visual odometer without 3d reconstruction for aerial vehicles. applications to building inspection," in *Proceedings of the 2005 IEEE International Conference on Robotics and Automation*, 2005.
[6] Barber D. B., Griffiths S. R., McLain T. W., Beard R. W., "Autonomous landing of miniature aerial vehicles," in *Proceedings of the AIAA Infotech@Aerospace Conference*, 2005.
[7] Meister O., Moenikes R., Wendel J., Frietsch N., Schlaile C., Trommer G. F., "Development of a GPS/INS/MAG Navigation System and Waypoint Navigator for a VTOL UAV," in *Proceedings of the SPIE Defense and Security Symposium*, vol. 6561, 2007.

[8] Meister O., Frietsch N., Ascher C., Trommer G. F., “Adaptive path planning for a vtol-uav,” in *Proceedings of the IEEE/ION Position Location and Navigation Symposium*, 2008.
[9] Lucas B. D., Kanade, T., “An Iterative Image Registration Technique with an Application to Stereo Vision,” in *Proceedings of Imaging Understanding Workshop*, 1981, pp. 121 – 130.
[10] Tomasi C., Kanade T., “Detection and Tracking of Point Features,” Carnegie Mellon University, Pittsburgh, Tech. Rep. CMU-CS-91-132, 1991.
[11] Harris C., Stephens M., “A combined corner and edge detector,” in *Proceedings of The Fourth Alvey Vision Conference*, 1988, pp. 147 – 151.
[12] Hartley R., Zisserman A., *Multiple View Geometry, Second Edition*. Cambridge: Cambridge University Press, 2003.
[13] Fischler M. A. and Bolles R. C., “Random Sample Consensus: A Paradigm for Model Fitting with Applications to Image Analysis and Automated Cartography,” *Communications of the ACM*, vol. 24, no. 6, pp. 381 – 395, 1981.
[14] Triggs B., “Autocalibration from planar scenes,” in *Extended version of paper in Proceedings of the 5th European Conference on Computer Vision ECCV*, vol. I, 1998, available via http://lear.inrialpes.fr/people/triggs/pubs/.
[15] Ma Y., Soatto S., Koseck J., Sastry S.S., *An Invitation to 3-D Vision*. New York: Springer, 2004.
[16] Frietsch N., Meister O., Schlaile C., Seibold J., Trommer G. F., “Vision based landing system for a vtol-mav,” in *Proceedings of NAV - The Navigation Conference & Exhibition*, 2008.